Genetic and structural validation of phosphomannomutase as a cell wall target in Aspergillus fumigatus

Zhang, Yuanwei; Fang, Wenxia; Raimi, Olawale G.; Lockhart, Deborah; Ferenbach, Andrew T.; Lu, Ling

Published in:
Molecular Microbiology

DOI:
10.1111/mmi.14706

Publication date:
2021

Received: 5 October 2020 | Revised: 3 February 2021 | Accepted: 15 February 2021

DOI: 10.1111/mmi.14706

RESEARCH ARTICLE

WILEY

Genetic and structural validation of phosphomannomutase as a cell wall target in *Aspergillus fumigatus*

Yuanwei Zhang [1,2] | Wenxia Fang [2,3] | Olawale G. Raimi [2] | Deborah E. A. Lockhart [2] | Andrew T. Ferenbach [2] | Ling Lu [1] | Daan M. F. van Aalten [2]

[1]Jiangsu Key Laboratory for Microbes and Functional Genomics, Jiangsu Engineering and Technology Research Centre for Microbiology, College of Life Sciences, Nanjing Normal University, Nanjing, China

[2]School of Life Sciences, University of Dundee, Dundee, UK

[3]National Engineering Research Center for Non-Food Biorefinery, Guangxi Academy of Sciences, Nanning, China

Correspondence
Daan M. F. van Aalten, School of Life Sciences, University of Dundee, Dundee DD1 5EH, UK.
Email: dmfvanaalten@dundee.ac.uk

Funding information
Medical Research Council, Grant/Award Number: V001094

Abstract

Aspergillus fumigatus is an opportunistic mold responsible for severe life-threatening fungal infections in immunocompromised patients. The cell wall, an essential structure composed of glucan, chitin, and galactomannan, is considered to be a target for the development of antifungal drugs. The nucleotide sugar donor GDP-mannose (GDP-Man) is required for the biosynthesis of galactomannan, glycosylphosphatidylinositol (GPI) anchors, glycolipid, and protein glycosylation. Starting from fructose-6-phosphate, GDP-Man is produced by the sequential action of the enzymes phosphomannose isomerase, phosphomannomutase (Pmm), and GDP-mannose pyrophosphorylase. Here, using heterokaryon rescue and gene knockdown approaches we demonstrate that the phosphomannomutase encoding gene in *A. fumigatus* (*pmmA*) is essential for survival. Reduced expression of *pmmA* is associated with significant morphological defects including retarded germination, growth, reduced conidiation, and abnormal polarity. Moreover, the knockdown strain exhibited an altered cell wall organization and sensitivity toward cell wall perturbing agents. By solving the first crystal structure of *A. fumigatus* phosphomannomutase (*Af*PmmA) we identified non-conservative substitutions near the active site when compared to the human orthologues. Taken together, this work provides a genetic and structural foundation for the exploitation of *Af*PmmA as a potential antifungal target.

KEYWORDS
Aspergillus fumigatus, crystal structure, drug target, phosphomannomutase

1 | INTRODUCTION

Aspergillus fumigatus is a ubiquitous and opportunistic filamentous fungus that causes life-threatening invasive aspergillosis with a high mortality rate in immunocompromised individuals such as bone marrow and solid organ transplant recipients (Brown et al., 2012; Kousha et al., 2011). The therapeutic options for *A. fumigatus* infections are restricted due to limited antifungal repertoire, severe side effects in patients and emergence of drug resistance (Bongomin et al., 2017; Robbins et al., 2017). Only four structural classes of antifungal drugs (azoles, polyenes, echinocandins, and flucytosine) are used in the clinical treatment of fungal infections (Ostrosky-Zeichner et al., 2010) and no novel antifungal classes have been discovered since 2006 (Denning & Bromley, 2015). Clinical development of novel therapeutics is mainly limited to combinations of existing drugs, repurposing medications or novel synthetic molecules with unknown mechanisms of action (Calderone et al., 2014). Thus, these problems highlight the importance of identifying and characterizing

new antifungal targets against *A. fumigatus* in order to feed into drug discovery pipelines.

The fungal cell wall is a complex and highly dynamic structure that is essential for cellular morphology and protection against environmental stresses and is considered to be a potential drug target. It is primarily composed of the polysaccharides chitin, glucan, and galactomannan (Gow et al., 2017; Latge et al., 2005). In *A. fumigatus*, galactomannan is a highly complex structure containing different types of glycosidic linkages, produced by several mannosyltransferases (Lee & Sheppard, 2016). As an active form of mannose, GDP-mannose is not only required for biosynthesis of fungal galactomannan, but also plays an important role in biosynthesis of O- and N-linked glycoproteins, glycosylphosphatidylinositol (GPI) anchors and glycolipids (Latge et al., 2017; Onoue et al., 2018). GDP-mannose biosynthesis is catalyzed by a cascade of three enzymes, starting from fructose 6-phosphate (Fru-6P), converted to mannose 6-phosphate (Man-6P) by mannose 6-phosphate isomerase (Pmi), isomerized to mannose 1-phosphate by phosphomannomutase (Pmm), and finally converted to GDP-mannose in the presence of GTP by GDP-mannose pyrophosphorylase (Gmp) (Sharma et al., 2014). Pmm, the second enzyme in GDP-mannose biosynthesis, belongs to the haloalkanoic acid dehalogenase (HAD) superfamily, containing a conserved phosphorylated motif DxDx(T/V) and utilizing a bisphosphate sugar (either glucose 1,6-bisphosphate or mannose 1,6-bisphosphate) as a co-factor (Allen & Dunaway-Mariano, 2004; Collet et al., 1998). Published crystal structures of Pmm from *Homo sapiens*, *Leishmania mexicana*, and *Candida albicans* revealed conserved overall structures with a similar catalytic mechanism of this enzyme family (Ji et al., 2018; Kedzierski et al., 2006; Silvaggi et al., 2006). Since GDP-mannose is a key metabolic intermediate for many cellular processes, Pmms have been identified and genetically characterized in eukaryotes. For example, *Saccharomyces cerevisiae* Pmm was shown to be essential for cell viability under in vitro laboratory conditions (Kepes & Schekman, 1988). Similar findings were observed in *Arabidopsis thaliana*, where failure of obtaining the *pmm* deletion and knockdown mutants indicated *pmm* essentiality. Reduced expression of *pmm* leads to a decrease in levels of the antioxidant ascorbic acid (AsA) and protein glycosylation (Hoeberichts et al., 2008). Mutants of *pmm* in the protozoan parasite *L. mexicana* are viable but avirulent (Garami et al., 2001). Furthermore, defects in *H. sapiens* Pmm2 result in a congenital disorder of glycosylation type 1a (CDG-1a), known as Jaeken syndrome, and early embryonic lethality whereas loss of Pmm1 is not implicated in any known pathology (Cromphout et al., 2006; Grunewald, 2009; Thiel et al., 2006; Westphal et al., 2001).

Antifungal drug development has historically been impeded by evolutionary similarities between fungi and their human host. Thus, characterizing the biological functions and structural properties of potential drug targets is an essential prerequisite for rational design of novel inhibitors (Hu et al., 2007). Structure-based drug discovery has been developed rapidly in the last two decades. Particularly, with the emergence of fragment-based drug discovery (FBDD) (Erlanson et al., 2016), it is possible to identify weakly binding small fragments (usually molecular mass < 300 Da) targeting binding sites away from highly conserved active sites. These fragments can be converted to potent inhibitors with high selectivity by iterative optimization based on structural and enzymological information (Scott et al., 2012). To date, although the function of phosphomannomutase has been well characterized in many eukaryotes, the physiological function of PmmA in the human opportunistic pathogen *A. fumigatus* remains unclear. Moreover, active site sequence conservation of this enzyme family with the human orthologues hampers the development of specific inhibitors. Here, we demonstrate that *Af*PmmA is indispensable for viability, morphogenesis, and cell wall integrity in *A. fumigatus*. Importantly, we reveal potential exploitable differences in *Af*PmmA structure compared to its human orthologues. This work forms the basis for the initiation of structure-based inhibitor design against *Af*PmmA.

2 | RESULTS

2.1 | *A. fumigatus* possesses a functional phosphomannomutase

Using the Genbank accession codes of *H. sapiens* Pmm1 (NP_002667.2) and Pmm2 (NP_000294.1) for a BLASTp search in *A. fumigatus* A1163 genome yielded a single putative phosphomannomutase (*Af*PmmA, EDP49225.1) corresponding to the *pmmA* gene (AFUB_072510). *A. fumigatus pmmA* is located on chromosome 6 and 1,087 bp in length containing four exons and three introns. The encoded protein *Af*PmmA contains 245 amino acids with 49% and 53% identity to human Pmm1 and Pmm2, respectively. *Af*PmmA is predicted to catalyze the conversion of mannose-6-phosphate (Man-6P) to mannose-1-phosphate (Man-1P) in the synthesis pathway of GDP–mannose (GDP-Man), which is the precursor for fungal cell wall mannan biosynthesis (Jin, 2012). To determine whether *Af*PmmA possesses phosphomannomutase activity, we overexpressed *Af*PmmA (residues 12–269) as a GST fusion protein in *Escherichia coli* yielding 8 mg per liter of pure *Af*PmmA after GST-tag cleavage and purification. Phosphomannomutases have been reported to use either Glc-1P or Man-1P as substrates (Pirard et al., 1999a, 1999b). To detect *Af*PmmA activity we used a coupled assay using glucose-6-phosphate dehydrogenase, phosphoglucose isomerase, and phosphomannose isomerase (for Man-1P) or glucose-6-phosphate dehydrogenase (for Glc-1P) as coupling enzymes (Figure 1a). Our data showed that *Af*PmmA had a K_m of 86 ± 11 μM for Glc-1P and a K_m of 26 ± 5 μM for Man-1P (Figure 1b,c). Compared to *Hs*Pmm1 (K_m for Glc-1P and Man-1P being 5.8 ± 0.8 μM and 54 ± 2 μM, respectively) (Silvaggi et al., 2006), *Af*PmmA is more selective for Man-1P. However, *Af*PmmA was 5-fold less catalytically efficient for Glc-1P (k_{cat}/K_m = 0.086 μM^{-1} s^{-1}) than *Hs*Pmm1 (k_{cat}/K_m = 0.38 μM^{-1} s^{-1}). The catalytic efficiency for Man-1P (k_{cat}/K_m = 0.054 μM^{-1} s^{-1})

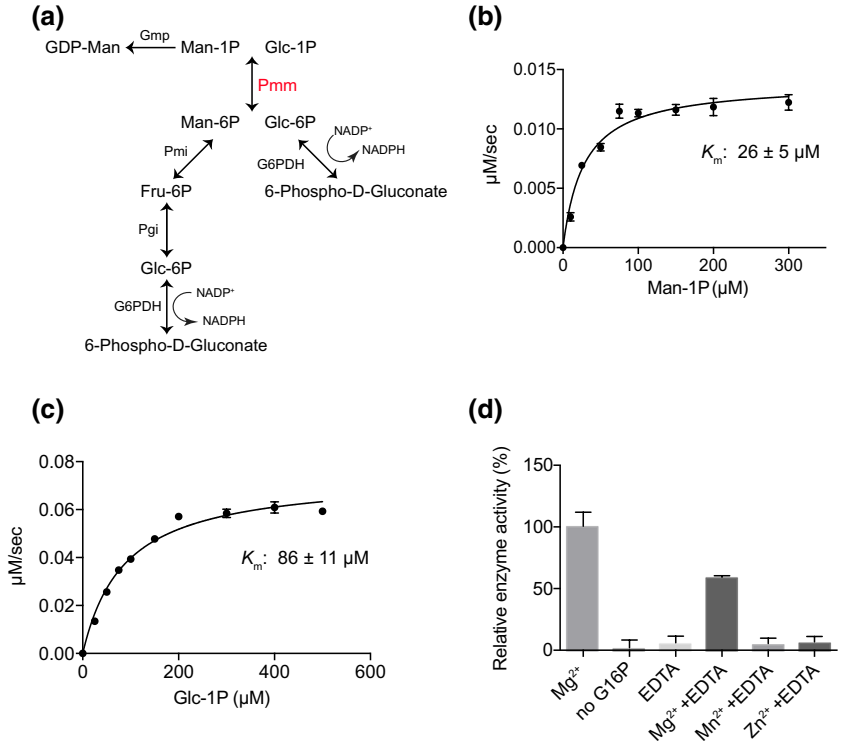

FIGURE 1 Kinetic analysis of recombinant *Aspergillus fumigatus* phosphomannomutase (*Af*PmmA). (a) Schematic illustrations of *Af*PmmA assays. Phosphoglucomutase assay: coupled assay with glucose-6-phosphate dehydrogenase (G6PDH) using Glc-1P as substrate. Phosphomannomutase assay: coupled assay with *A. fumigatus* phosphomannose isomerase (Pmi) and phosphoglucose isomerase (Pgi) using Man-1P as substrate. (b,c) Kinetic parameters of *Af*PmmA catalyzed conversion of Glc-1P to Glc-6P (b) or Man-1P to Man-6P (c) in 50 mM HEPES pH 7.1, 5 mM $MgCl_2$, 0.25 mM $NADP^+$ by monitoring NADPH production. 10 μM Glc-1,6-bisP was used as cofactor. The results are the mean ± *SD* for three determinations. (d) Effect of Glc-1,6-bisP, EDTA and metal ions on *Af*PmmA activity. The metal ions were added at 5 mM concentration and the activities were measured using 200 μM Glc-1P as substrate. Control indicates 10 μM Glc-1,6-bisP and 5 mM Mg^{2+} were added but without addition of EDTA or other metal ions

TABLE 1 Michaelis-Menten kinetics of *Af*PmmA/*Hs*Pmm1 and point mutants

Substrate	Enzyme	k_{cat} (s^{-1})	K_m (μM)	k_{cat}/K_m ($\mu M^{-1}\ s^{-1}$)
Man-1P	WT *Af*PmmA	1.4	26 ± 5	0.054
	*Hs*Pmm1	4.4	54 ± 2	0.081
	*Af*PmmA D25N	n.d.	n.d.	n.d.
	*Af*PmmA D27N	n.d.	n.d.	n.d.
Glc-1P	WT *Af*PmmA	7.4	86 ± 11	0.086
	*Hs*Pmm1	2.9	7.5 ± 0.8	0.38
	*Af*PmmA D25N	0.03	48 ± 9	0.0006
	*Af*PmmA D27N	0.03	79 ± 11	0.0004

Note: Data shown is the mean ± *SD* of three determinations, n.d. represents not detectable. The kinetics data of *Hs*Pmm1 were obtained from (Silvaggi et al., 2006).

was comparable to *Hs*Pmm1 (k_{cat}/K_m = 0.081 $\mu M^{-1}\ s^{-1}$) (Table 1). Like other eukaryotic phosphomannomutases, *Af*PmmA requires glucose-1,6-bisphosphate (Glc-1,6-bisP, a phosphorylation activator) and Mg^{2+} for activity (Allen & Dunaway-Mariano, 2004; Qian et al., 2007) (Figure 1d). Taken together, these data suggest that *A. fumigatus* possesses a functional phosphomannomutase.

2.2 | *AfpmmA* is essential for *A. fumigatus* viability in vitro

To investigate the role of *pmmA* in *A. fumigatus*, we attempted to construct a null mutant using the *Neurospora crassa pyr-4* selectable marker to replace the open reading frame of *AfpmmA* by homologous recombination (Figure 2a). However, we failed to obtain any positive transformants, suggesting that *AfpmmA* may be essential for growth under in vitro laboratory conditions. To further confirm essentiality of *AfpmmA*, a heterokaryon rescue technique was employed (Osmani et al., 2006). As shown in Figure 2b, all heterokaryons were not viable on selective media (YAG) but were able to grow on nonselective (YUU) media. Moreover, PCR analysis showed that these heterokaryons contained both wild type and deleted alleles (Figure 2c), indicating that *pmmA* is an essential gene in *A. fumigatus* which is consistent with previous studies in *S. cerevisiae* and *Kluyveromyces lactis* (Kepes & Schekman, 1988; Staneva et al., 2004). As an alternative strategy, we constructed a conditional inactivation mutant by replacing the native promoter of the *pmmA* gene with the *Aspergillus nidulans* alcohol dehydrogenase promoter (P_{alcA}) that is inducible by ethanol, glycerol, or threonine and repressed by glucose (Romero et al., 2003). Over fifty transformants were obtained and genotyped. The correct

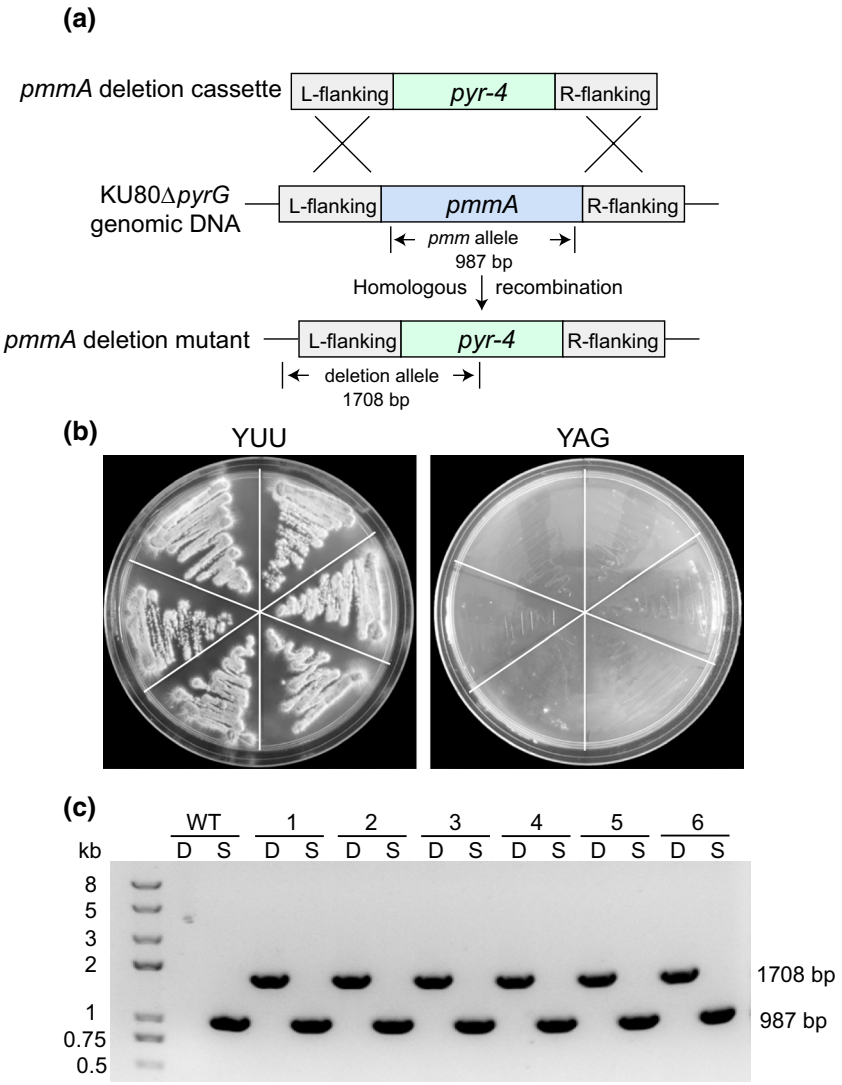

FIGURE 2 Heterokaryon rescue analysis of *AfpmmA* deletion strains. (a) The scheme of construction of the *AfpmmA* deletion strain. (b) After transformation with *pmmA* deletion cassette, conidia from six primary transformants were streaked onto selective (YAG) and nonselective (YUU) plates and grown for 48 hr at 37°C. (c) Heterokaryons were verified by diagnostic PCR. The wild-type only contains the wild-type allele (S, 987 bp, primers P19/P20) and that the all six heterokaryons contain both wild-type (S, 987 bp, primers P19/P20) and deletion alleles (D, 1708 bp, primers P21/P22)

conditional mutant was confirmed by diagnostic PCR and Southern blot (Figure S1). Both the wild type and *AfpmmA* conditional mutant (referred to as P_{alcA}::*pmmA*) displayed similar growth under inducing condition using minimal media (MM) supplemented with 0.1 M glycerol, 0.1 M ethanol, or 0.1 M threonine as carbon sources. In contrast, hyphal growth of P_{alcA}::*pmmA* was completely inhibited on YEPD and CM, suggesting that expression of *pmmA* is required for *A. fumigatus* viability (Figure 3a). The growth of P_{alcA}::*pmmA* was partially inhibited on MM containing 1% and 2% glucose (w/v) and 0.1 M threonine (Figure 2a). Quantitative PCR was utilized to determine the knockdown level of P_{alcA}::*pmmA* under partial repression and full induction conditions. The mRNA level of *pmmA* was identical compared to that of the wild type under inducing condition (MM with 0.1 M threonine [MMT]) and reduced to 56% of the wild type level under partial repression condition (MM with 0.1 M threonine and 1% glucose [MMTG], Figure 3b). Under MMTG, expression of *pmmA* was reduced to a minimum level that supports sufficient mycelia for subsequent experiments. Taken together, these data suggest that *pmmA* is essential for *A. fumigatus* viability in vitro.

2.3 | *pmmA* is required for morphogenesis in *A. fumigatus*

When grown under solid MMTG the radial hyphal growth of the P_{alcA}::*pmmA* conditional strain was decreased to approximately 45% of that of the wild type at each time point investigated, indicating in vitro growth was affected by the repression of *pmmA* (Figure 4a). Apart from this, the P_{alcA}::*pmmA* conditional strain also showed reduced conidiation under repressive conditions (Figure 4b). We next used differential interference contrast (DIC) microscopy to examine the edges of the colonies under inducing and repressing conditions. An abnormal morphological phenotype of hyper-branching at the hyphal tips was observed when *pmmA* is repressed (Figure 4c).

To further explore the effect of *pmmA* repression in *A. fumigatus*, the germination rate and pattern were investigated under the repressing condition. The P_{alcA}::*pmmA* conditional strain displayed 8 hr delayed germination comparing to the wild type (Figure 5a). Moreover, a defective germination pattern was observed for the P_{alcA}::*pmmA* conditional strain with 22% morphological abnormalities

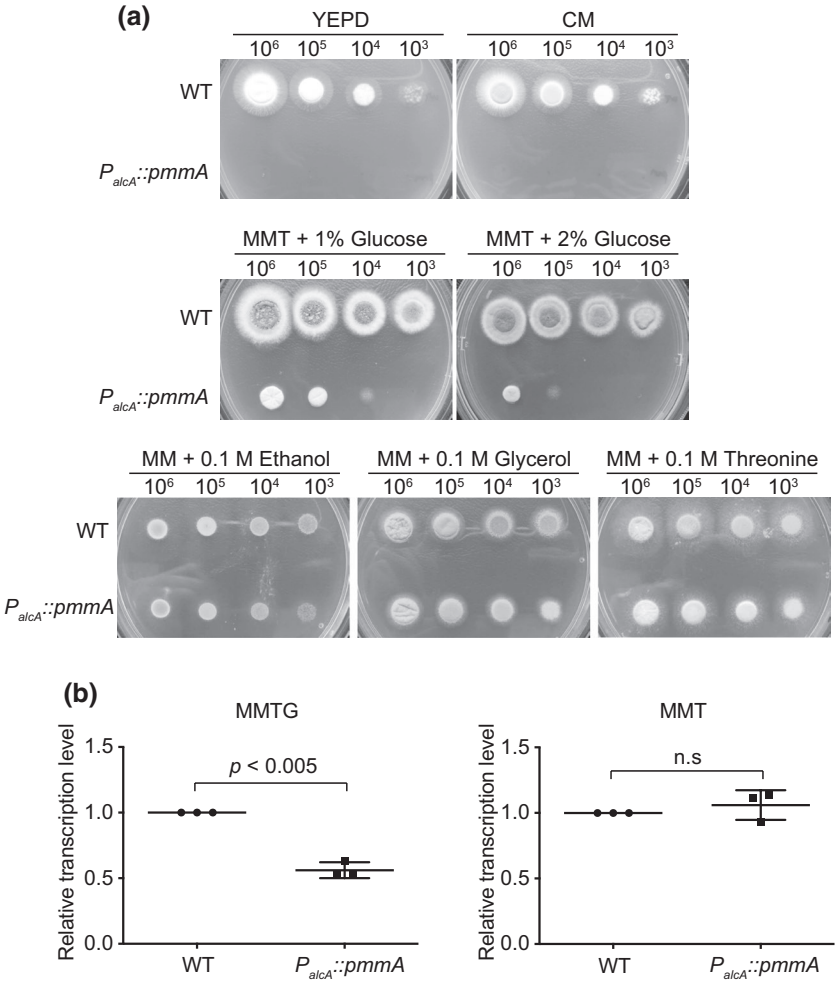

FIGURE 3 Growth phenotype of the P_{alcA}::*pmmA* conditional mutant under inducing and repressing growth conditions. (a) A series of 10-fold dilutions of the indicated strains were inoculated at 37°C for 48 hr on YEPD, CM, and MM supplemented with 1% and 2% glucose (w/v), 0.1 M ethanol, 0.1 M glycerol, 0.1 M threonine. (b) Relative transcription level of *AfpmmA* gene under induction (MMT) and partial repression (MMTG, MMT with 1% glucose) conditions. Gene expression levels were normalized to the reference gene *tbp*. Error bars indicate mean ± *SD* from three independent experiments. Data were analyzed using an unpaired of *t*-test, statistical significance is indicated by *p* values; ns, not significant

in loss of polarity and a high frequency of apical branching at hyphal tips (Figure 5b,c) whereas 92% of the wild type cells formed a single, straight germ tube and 8% forming two germ tubes ($n = 200$). Taken together, these results suggest that repression of *pmmA* results in a pronounced defect in polarity establishment that is required for hyphal growth and asexual development. Thus, *pmmA* is required for morphogenesis in *A. fumigatus*.

2.4 | *AfpmmA* expression affects *A. fumigatus* cell wall organization and secreted protein glycosylation

Previous studies demonstrated that enzymes involved in sugar nucleotide biosynthetic pathways are required for cell wall integrity in fungi. For example, deficiency of UDP-N-acetylglucosamine pyrophosphorylase (Uap1) (Fang et al., 2013b), N-acetylphosphoglucosamine mutase (Agm1) (Fang et al., 2013a), phosphoglucose isomerase (Pgi) (Upadhyay & Shaw, 2006; Zhang et al., 2015), UDP-glucose pyrophosphorylase (Ugp) (Li et al., 2015), Phosphomannose isomerase (PMI) (Fang et al., 2009), and GDP-mannose pyrophosphorylase (Gmp) (Jiang et al., 2008) lead to the alteration of cell wall components and cell wall deficiency. We investigated the role of *Af*PmmA in maintaining cell wall integrity by examining the sensitivity of the P_{alcA}::*pmmA* conditional mutant toward cell wall perturbing agents such as Calcofluor White (CFW), Congo red (CR), and Caspofungin. CFW and CR interfere with the cell wall structure by inhibiting the enzymes involved in connecting chitin to β-1,3-glucan and β-1,6-glucan (Ram & Klis, 2006) whereas Caspofungin inhibits the synthesis of β-1,3-glucan (Kahn et al., 2006). Repression of *pmmA* caused hypersensitivity of the P_{alcA}::*pmmA* conditional mutant to CR and CFW but did not alter sensitivity to Caspofungin (Figure 6a) whereas no change in sensitivity was observed under conditions inducing *pmmA* expression (Figure 6b). Moreover, the conidiation defect and susceptibility to CR and CFW of the P_{alcA}::*pmmA* conditional mutant can be significantly rescued by the addition of osmotic stabilizers (1.2 M sorbitol and 0.6 M KCl) to the repression medium, suggesting defects in cell wall integrity under *pmmA* repression conditions (Figure S2). Next, to test whether the phenotypic defects with cell wall perturbing agents were due to changes in the cell wall, we examined hyphal cell wall ultrastructure of wild type and the P_{alcA}::*pmmA* mutant by transmission electron microscopy (TEM). As shown in Figure 6c,d, the P_{alcA}::*pmmA* conditional mutant showed a much thinner cell wall compared to the wild type under repressing conditions. In contrast, no difference was observed between the wild type and conditional mutant with the induction of *pmmA* expression (Figure 6c,d). Moreover, we quantified the individual cell wall

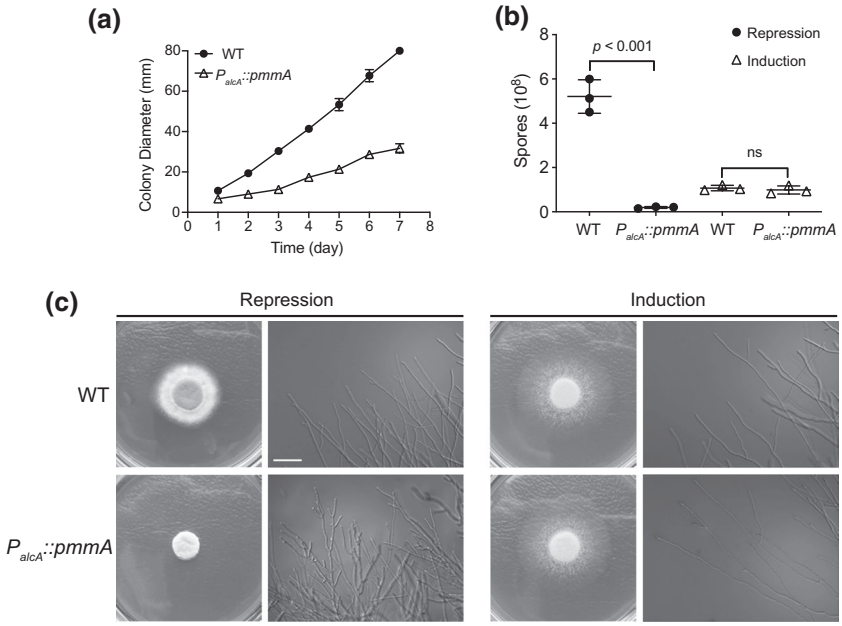

FIGURE 4 Phenotypic characterization of the P_{alcA}::*pmmA* conditional mutant. (a) 1 x 10^6 conidia from the indicated strains were inoculated onto solid partial repression (MMTG) media at 37°C, and colony diameter was measured daily. Data are presented as an average for each time points from three replicates ± standard deviation. (b) Quantitative data for the number of conidia of each strain grown on indicated medium for 48 hr at 37°C. Data are presented as an average from three replicates ± standard deviation. Data were analyzed using an unpaired of *t*-test, statistical significance is indicated by *p* values; ns, not significant. (c) Colonial and hyphal morphology of the indicated strains grown on solid partial repression (MMTG) or induction (MMT) media for 48 hr at 37°C. Scale bar represents 20 μm

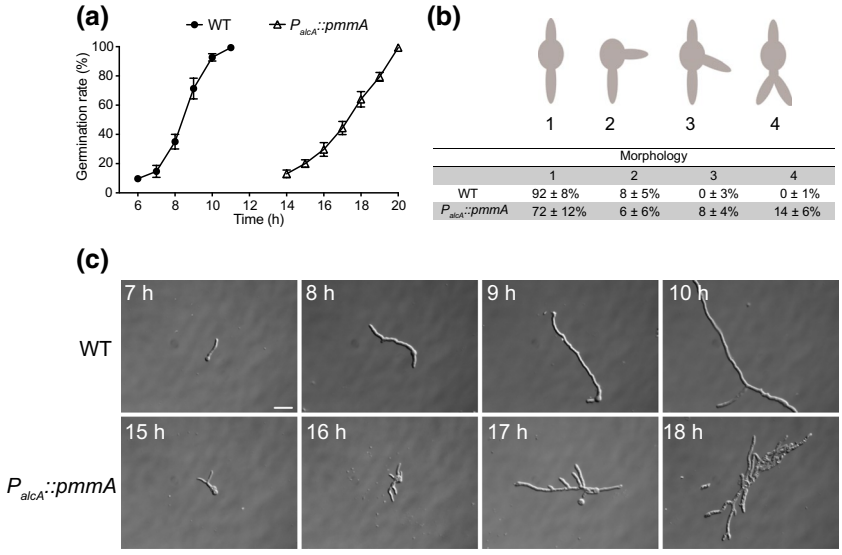

	Morphology			
	1	2	3	4
WT	92 ± 8%	8 ± 5%	0 ± 3%	0 ± 1%
P_{alcA}::*pmmA*	72 ± 12%	6 ± 6%	8 ± 4%	14 ± 6%

FIGURE 5 Conidial germination is affected by repression of *AfpmmA*. (a) Germination rate of the *AfpmmA* conditional mutant and the wild type. Conidia (1 × 10^6) were incubated in liquid partial repression (MMTG) media for the time indicated. One hundred conidia for each strain were assessed for germination rate and the experiment was performed in triplicate. Values represent the mean ± *SD*. (b) Germination pattern of the P_{alcA}::*pmmA* conditional mutant and the wild-type conidiospores. 1 × 10^6 conidia of the conditional mutant and the wild type were allowed to germinate in liquid partial repression (MMTG) media for 9 hr and 24 hr, respectively. Germination morphology was classified (1–4) as shown in figure. The experiment was performed in triplicate. Values represent the mean ± *SD*. (c) 1 × 10^6 conidia from each strain were inoculated into 2 ml liquid partial repression (MMTG) medium for the indicated time point at 37°C and examined by differential interference contrast (DIC) using Axio Scope A1 (Zeiss). Scale bar represents 20 μm

components of the wild type and P_{alcA}::*pmmA* mutant strains by high-performance ionic chromatography (Francois, 2006). Repression of *pmmA* expression led to the reduction of the galactose and mannose content by 56% and 57%, respectively, whereas the amounts of chitin and glucan were increased by 47% and 49%, respectively (Figure 7a). The cell wall components of the *pmmA* conditional strain

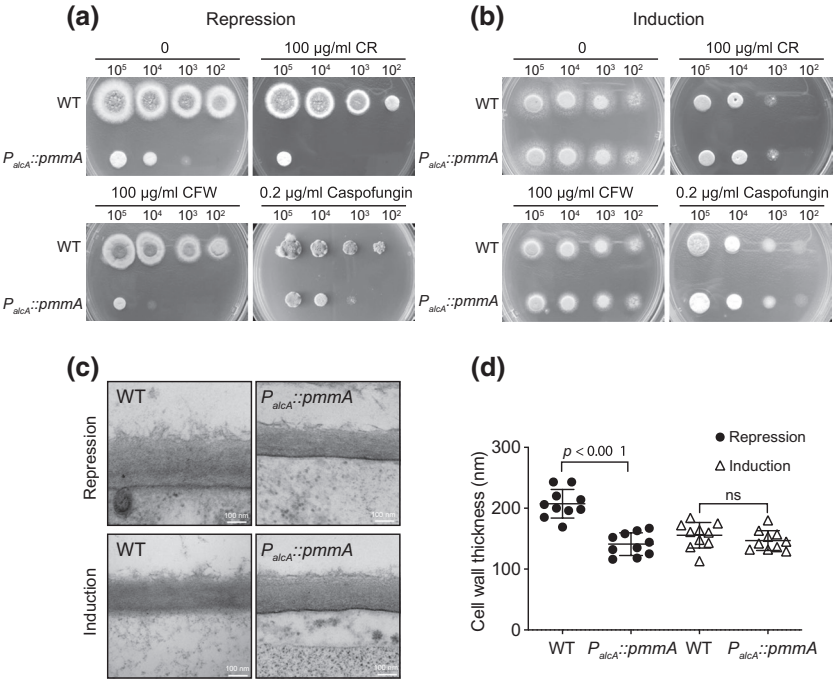

FIGURE 6 Sensitivity of the P_{alcA}::*pmmA* conditional strain to cell wall perturbing agents. (a,b) The indicated number of conidia were inoculated onto solid partial repression (MMTG) (panel a) and induction (MMT) (panel b) media supplemented with different cell wall perturbing agents: 100 μg/ml Congo Red (CR), 100 μg/ml Calcofluor White (CFW), and 0.2 μg/ml Caspofungin, and then were incubated at 37°C for 48 hr. (c) The transmission electron microscope (TEM) images of the wild type and *pmmA* conditional mutant hyphae in partial repression (MMTG) and induction (MMT) media. Scale bar represents 100 nm. (d) Quantification of the cell wall thickness of the wild type and *pmmA* conditional mutant hyphae from TEM images in respective conditions. Values represent the mean ± *SD* of 10 sections of different hyphae; Data were analyzed using an unpaired of *t*-test, statistical significance is indicated by *p* values; ns, not significant

were similar to those in the wild type upon induction of *pmmA* expression (Figure 7a). As GDP-Man is not only important for cell wall integrity but also involved in protein glycosylation, we extracted the total and secreted proteins from the wild type and P_{alcA}::*pmmA* conditional mutant to detect protein glycosylation levels by western blot using biotinylated Concanavalin A. As shown in Figure 7b, the repressed P_{alcA}::*pmmA* conditional mutant exhibited reduced glycosylation levels in secreted proteins, whereas no significant change was observed for intracellular proteins, suggesting that repression of *Af*PmmA leads to a reduction of secreted mannosylated proteins. Collectively, these results show that *AfpmmA* expression affects *A. fumigatus* cell wall organization and secreted protein glycosylation.

2.5 | The *Af*PmmA crystal structure reveals exploitable differences

Our data so far suggest that *Af*PmmA is a genetically validated antifungal target in *A. fumigatus*. However, the high sequence conservation to the human orthologues suggests that mechanism-inspired inhibitors could elicit toxicity. We next determined the crystal structure of *Af*PmmA to find potential exploitable differences compared to *Hs*Pmm1 and *Hs*Pmm2. Purified recombinant *Af*PmmA from *E. coli* was crystallized in PEG solutions in the presence of Mg^{2+}. Molecular replacement and refinement against 2.2 Å synchrotron diffraction data yielded a model with statistics as shown in Table 2. The $P2_12_12_1$ asymmetric unit consists of two dimers that have different conformations, with RMSDs of 1.7–2.7 Å for the four monomers versus the structure of *Hs*Pmm1 (PDB entry 2FUE, Silvaggi et al., 2006). However, superposition of the individual core and cap domains of *Af*PmmA onto the corresponding domains of the *Hs*Pmm1 (Silvaggi et al., 2006) yields RMSDs < 1.0 Å on Cα atoms. Since there is no evidence of half-site reactivity or cooperativity for this enzyme (Ji et al., 2018), a single monomer will be used in the description and figures herein.

The overall crystal structure of *Af*PmmA is similar to that of *C. albicans* Pmm (PDB entry 5UE7) (67% sequence identity, RMSD of 2.5 Å on 221 Cα atoms) and *L. mexicana* Pmm (PDB entry 2I54, (Kedzierski et al., 2006) (53% sequence identity, RMSD of 1.4 Å on 221 Cα atoms). The structure is divided into two domains: a core Rossman-fold domain (Rao & Rossmann, 1973) comprising five parallel β-sheets flanked by seven α-helices (residues 1–98 and 204–263), and a cap domain comprising residues 99–203. The cap and core domains are connected by hinge regions comprising residues 92–102 and 193–199 (Figure 8a). In order to dissect substrate binding modes, we attempted to soak or co-crystallize *Af*PmmA with a range of substrates including Man-1P, Man-6P, and Glc-1,6-bisP, but were unable to obtain any complex. By sequence alignment with human phosphomannomutases, the key active site residues in the *Af*PmmA are Asp25 as the catalytic nucleophile and Asp27 as an acid

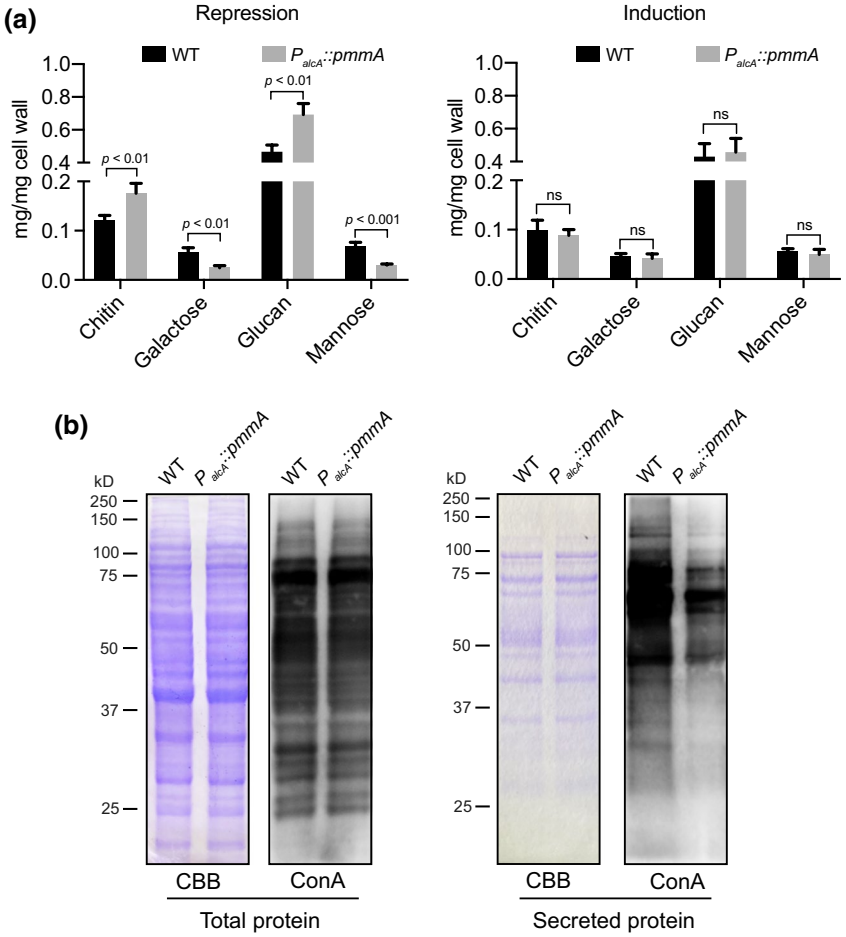

FIGURE 7 Cell wall monosaccharide contents and glycosylated proteins of the P_{alcA}::*pmmA* conditional mutant compared to the wild type. (a) 1×10^6 conidia were incubated in 100 ml liquid partial repression (MMTG) (left panel) and induction (MMT) (right panel) media at 37°C for 48 hr. The mycelia were harvested and 10 mg dry mycelium samples were used for analysis as described in Experimental procedures. Measurements were performed in three independent replicates with six technical replicates. Data were analyzed using an unpaired of *t*-test, statistical significance is indicated by *p* values; ns, not significant. (b) Western analysis of total proteins and secreted proteins from the wild-type strain and *pmmA* conditional mutant using a biotinylated ConA antibody. Coomassie brilliant blue (CBB) staining was used as the protein loading control

catalyst in the transfer of the phosphoryl group to the Asp25 nucleophile (Figure S3). To detect whether these residues are required for *Af*PmmA catalytic activity, we performed site-directed mutagenesis to create two distinct point mutants (D25N and D27N) and assessed their kinetic properties. The results showed that catalytic efficiency of D25N and D27N for Glc-1P decreased 87-fold and 130-fold, respectively, when compared to wild type *Af*PmmA (Table 1). Enzymatic activity was completely abolished for Man-1P, suggesting that these residues are critical for catalytic activity of *Af*PmmA. As a member of the β-D-phosphohexomutase superfamily a conserved aspartate, corresponding to Asp25 in *Af*PmmA, was proposed as a nucleophile to form a transient phosphoenzyme intermediate (Jin et al., 2014). However, we did not see crystallographic evidence of phosphorylation of Asp25, which is in agreement with the reports on human and *L. mexicana* Pmm structures (Kedzierski et al., 2006; Silvaggi et al., 2006). This is likely due to the fact that aspartic acid is only transiently phosphorylated during catalysis.

Structural superposition of *Af*PmmA with the structure of *Hs*Pmm1 in complex with Man-1P revealed a high level of similarity, with the amino acids required for substrate binding and catalysis being conserved. While Asp231 and Lys232 in *Af*PmmA, which coordinate the magnesium ion, correspond to Asn218 and Glu219 in *Hs*Pmm1, they are conserved as Asp231 and Lys232 in *Hs*Pmm2 (Figures 8b and S3). Similarly, the active site residue Gln193 in *Af*PmmA is equivalent to Met186 in *Hs*Pmm1 and Gln177 in *Hs*Pmm2 (Figures 8c and S3). Although the catalytic machinery of *Af*PmmA and human phosphomannomutases is fully conserved, a close inspection of both active site and substrate binding areas reveals that the human and fungal phosphomannomutases possess potentially exploitable differences (Figure 8d). For instance, Glu28 in *Af*PmmA near the active site is equivalent to Gly22 and Gly15 in *Hs*Pmm1 and *Hs*Pmm2, respectively. Residues near the Man-1P binding site, Arg35 and Ala36 in *Af*PmmA, are equivalent to Gln29 and Lys30 in *Hs*Pmm1 and Gln22 and Lys23 in *Hs*Pmm2, respectively. Thus, *Af*PmmA possesses potentially exploitable differences compared to the human orthologues.

3 | DISCUSSION

In order to circumvent resistance and treat infections of the opportunistic pathogen *A. fumigatus*, the development of novel antifungals targeting critical cellular components or biological mechanisms is urgently needed (Denning & Bromley, 2015). Enzymes participating in fungal cell wall biogenesis present attractive drug targets due to their essential biological roles. For instance, the antifungal drug class echinocandins target β-1, 3-glucan synthase, a key enzyme essential for cell wall integrity. Several lines of evidence suggest that GDP-mannose, the donor substrate for biosynthesis of cell wall mannan, O/N-glycans, and GPI anchors, plays an important role in fungal growth and development

TABLE 2 Data collection and structure refinement

	*Af*PmmA
Resolution (Å)	23.0–2.2 (2.32–2.20)
Space group	$P2_12_12_1$
Unit cell (Å)	$a = 80.5$, $b = 102.1$, $c = 137.8$
No. of reflections	203,250 (26,985)
No. of unique reflections	56,365 (7,848)
I/σ (I)	5.7 (2.9)
Completeness (%)	98.9 (90.0)
Multiplicity	3.6 (3.4)
R_{merge}	0.149 (0.363)
RMSD from ideal geometry	
Bonds (Å)	0.015
Angles (°)	1.69
R_{work} (%)	19.6
R_{free} (%)	24.2
No. of residues	1,041
No. of water mol.	975
B factors (Å^2)	
Overall	18.7
Protein	18.0
Ligand	25.1
Solvent	24.1
PDB entry	6I5X

Note: Data between brackets represent the highest resolution shell.

(Bernard & Latge, 2001; Bowman & Free, 2006; De Groot et al., 2005). However, studies regarding the biological functions and structural properties of the enzymes in the GDP-mannose biosynthesis pathway are limited. In this study, with the combination of genetic and structural characterizations, we propose that the *A. fumigatus* phosphomannomutase PmmA could be a potential drug target.

Several genetic studies have demonstrated that Pmm is indispensable for viability in many eukaryotes (Hoeberichts et al., 2008; Kepes & Schekman, 1988; Staneva et al., 2004). In agreement, heterokaryon rescue and phenotypic analysis of a conditional mutant employing the *alc(A)* promoter confirmed that *pmmA* is an essential gene in *A. fumigatus* (Figures 2 and 3). Reduced expression of *AfpmmA* resulted in pleiotropic phenotypes such as retarded vegetative growth, decreased conidiation, and abnormal hyphal branching in *A. fumigatus* (Figures 4 and 5). Similar phenotypic defects were observed in several studies with galactomannan deficiency mutants including mannosyltransferases Ktr4/CmsA, Ktr7/CmsB, and GDP-mannose transporter GmtA in *A. fumigatus* (Engel et al., 2012; Henry et al., 2019; Onoue et al., 2018). Moreover, the downstream enzyme of the GDP-mannose pathway, GDP-mannose pyrophosphorylase (Gmp) is also essential for viability of *A. fumigatus* (Jiang et al., 2008). *gmp* deficiency induced similar phenotypes as the *pmmA* repression mutant with the exception of early germination. A possible explanation is that reduced expression of *gmp* only affects GDP-mannose synthesis, while repression of *pmmA* mutant may lead to the limitation of UDP-glucose since Pmm is also able to convert Glc-1P to Glc-6P, the precursor of UDP-glucose. In addition to the defects in hyphal growth, *AfpmmA* conditional mutants exhibited alterations of cell wall architecture, decreased galactomannan content, and increased chitin and glucan content under partial repressing conditions (Figures 6 and 7). However, the compensatory increased content of chitin and glucan is not sufficient to maintain normal hyphae growth when *AfpmmA* is repressed. Supplementation with osmotic stabilizers could rescue the conidiation defects and sensitivity toward cell wall perturbing agents but not hyphal growth in the *pmmA* conditional mutant, suggesting that the abnormal hyphal growth and polarity may not be exclusively due to cell wall integrity defects. Although we have not examined intracellular hexose phosphate metabolites such as Man-1P, Man-6P, GDP-mannose in the *AfpmmA* conditional mutant, A reduction of secreted protein glycosylation was observed when *AfpmmA* is repressed. Moreover, a previous study on *A. fumigatus* phosphomannose isomerase (Pmi), the enzyme upstream of PmmA in GDP-mannose biosynthesis, revealed that deletion of *Afpmi* leads to abnormal intracellular hexose phosphates homeostasis (Fang et al., 2009). It is thus possible that the phenotypes observed in the *AfpmmA* deficiency mutant are a consequence of the decreased intercellular pools of GDP-mannose. For instance, increased susceptibility of the *AfpmmA* conditional mutant to ER stress suggests that repression of *Af*PmmA may globally affect GPI-anchor synthesis (Figure S2c), which could lead to defects in the delivery and sorting of components required for polarity of hyphal tips.

Microbial virulence results from the interaction between the microbe and the host, with the host immune response being critical for the establishment of infection (Casadevall & Pirofski, 2003). The fungal cell wall acts as the outermost barrier mediating interaction with the environment and mammalian host cells. The composition and structure of the cell wall are critical for the activation of the immune response during infection. Previous studies have shown that deficiencies in galactomannan and protein O-/N-glycosylation results in attenuated virulence and altered host immune response (Barreto-Bergter & Figueiredo, 2014). The physiological effects of alterations in the cell wall due to *AfpmmA* repression in the context of a host requires further investigation.

Enzyme kinetics of *Af*PmmA showed that the Mg^{2+}-dependent enzyme possesses both phosphoglucomutase and phosphomannomutase activity with different rate constants (Figure 1). The reaction mechanism of phosphomannomutases has been well characterized (Nogly et al., 2013; Seifried et al., 2013). An aspartic acid catalytic nucleophile initiates a nucleophilic attack on the phosphoryl group of the substrate, generating a phosphoaspartyl intermediate, followed by nucleophilic attack of a water molecule on the phosphoaspartyl intermediate to regenerate the catalytic Asp (Seifried et al., 2013). A Glc-1,6-bisP cofactor is required for maintaining the active site of this family of enzymes in the phosphorylated state (Knowles, 1980). In this work, there was no electron density for the phosphorylation of the *Af*PmmA active site Asp25, in line with the absence of *Af*PmmA activity in the absence of Glc-1,6-bisP (Figure 1d).

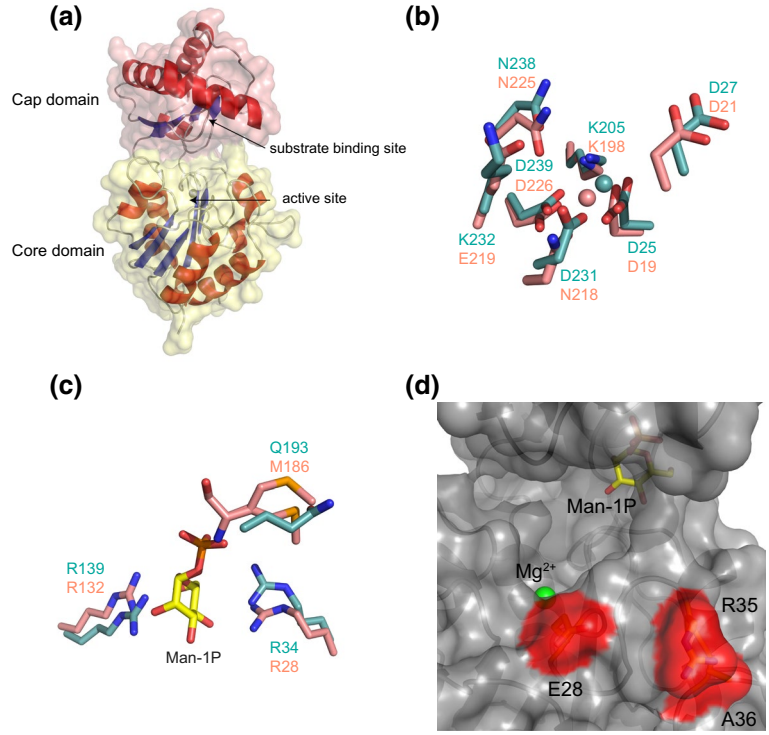

FIGURE 8 Crystal structure of *Af*PmmA. (a) Overview of the *Af*PmmA crystal structure. Cap domain and core domain are colored in salmon and yellow, respectively. Secondary-structure elements of each domain are colored red (helices) and blue (strands). Mg^{2+} ions are shown as grey spheres. (b,c) Superposition of the Mg^{2+} binding site (b) and Man-1P binding site (c) residues in the *Hs*Pmm1-Man-1P complex (PBD entry 2FUE, Silvaggi et al., 2006) with the corresponding residues in *Af*PmmA. Carbon atoms of residues are shown as salmon (*Hs*Pmm1) and teal (*Af*PmmA) sticks. Mg^{2+} ions from *Hs*Pmm1 and *Af*PmmA are colored in salmon and teal spheres, respectively. The predicted position of Man-1P was obtained by superposition with *Hs*Pmm1-Man-1P complex (PBD entry 2FUE, Silvaggi et al., 2006) and shown as sticks with yellow carbon atoms. (d) Close-up view of the *Af*PmmA active site. Conserved residues with *Hs*Pmm1 are colored in grey, non-conserved substitutions are colored in red. Mg^{2+} is shown as a green sphere. The predicted position of Man-1P was obtained by superposition with *Hs*Pmm1-Man-1P complex (PBD entry 2FUE, Silvaggi et al., 2006) and shown as sticks with yellow carbon atoms

Compounds targeting essential genes such as *pmmA* may have substantial toxicity due to evolutionary conserved enzymatic properties and the high structural similarity with its human orthologues. To date, information on inhibitors of this class of enzymes is limited to a single report describing the dye Disperse Blue 56 (2-chloro-1,5-diamino-4,8-dihydroxyanthraquinone) that was identified by virtual screening as an aggregating inhibitor of *Pseudomonas aeruginosa* α-D-phosphohexomutase (Pmm/Pgm) (Liu et al., 2004). The high-resolution crystal structure of *Af*PmmA reveals that it shares a fold with other members of phosphomannomutase superfamily (Figure 8a). By superposition of the *Af*PmmA with *Hs*Pmm1-Man-1P complex structure, we identified that the *Af*PmmA possesses three non-conserved residues near the Mg^{2+} and Man-1P binding sites (Figure 8d). With the advent of fragment-based drug discovery (Scott et al., 2012) and PROTAC (Proteolysis targeting chimera) technology (Zou et al., 2019), it is possible to exploit and identify molecules with selectivity based on subtle differences in protein structure and even for undruggable targets. For instance, inhibitors have been developed against other enzymes involved in sugar nucleotide biosynthesis, such as N-acetylphosphoglucosamine mutase *Af*Agm1 (Fang et al., 2013a), glucosamine 6-phosphate N-acetyltransferase *Af*Gna1 (Lockhart et al., 2020), and N-acetylglucosamine pyrophosphorylase Uap1 in *A. fumigatus* and *Trypanosoma brucei* (Fang et al., 2013b; Urbaniak et al., 2013). Similarly, although N-myristoyltransferase (Nmt) from *Plasmodium falciparum* only displays a single residue difference at the active site from human Nmt, selective inhibitors have been successfully identified and further optimized (Bell et al., 2012; Rackham et al., 2014). Thus, it is possible to develop potent selective inhibitors against *Af*PmmA based on the structure differences from human Pmms we presented here.

In conclusion, the genetic and structural analysis of PmmA in *A. fumigatus* reported here suggests that *Af*PmmA is a potential target for the development of antifungal drugs. Future efforts are required to discover inhibitors targeting this key enzyme in cell wall biosynthesis that may possess anti-fungal activity.

4 | EXPERIMENTAL PROCEDURES

4.1 | Strains and culture conditions

A. fumigatus Ku80Δ*pyrG* was the recipient parental strain for generating the mutants described in this work (da Silva Ferreira et al., 2006).

Minimal medium (MM) supplemented with 0.1 M glycerol, 0.1 M threonine or 0.1 M ethanol as carbon sources was used to induce gene expression. YEPD (2% w/v yeast extract, 2% w/v glucose and 0.1% w/v peptone) medium and CM (complete medium) were used to completely and partially repress gene expression (Armitt et al., 1976; d'Enfert, 1996). YAG (2% w/v glucose, 0.5% w/v yeast extract, trace elements and 2% w/v agar) and YUU (YAG supplemented with 1.2 g/L each of uracil and uridine) were used for heterokaryon rescue assays. (Todd et al., 2007). *A. fumigatus* conidia were grown on minimal medium at 37°C for 48 hr and harvested in sterile water supplemented with 0.02% (v/v) Tween 20, and counted in a hemocytometer. Conidia were stored in 20% glycerol stock at −80°C for long-term storage or in sterile water at 4°C for short term storage.

4.2 | Heterokaryon rescue

Heterokaryon rescue assays were performed as previously described (Osmani et al., 2006). Conidia from heterokaryotic primary transformants were replica streaked onto selective (YAG) and nonselective (YUU) plates for the *pyrG* marker of the *pmm* deletion cassette. Heterokaryons were confirmed by diagnostic PCR using primer P19/P20 for wild-type alleles and primers P21/P22 for deletion alleles.

4.3 | Construction of the *A. fumigatus pmmA* conditional inactivation mutant

The pAL3 plasmid (Romero et al., 2003) containing the alcohol dehydrogenase promoter (P_{alcA}) and the *N. crassa pyr-4* gene as a fungal selectable marker was used to construct a vector allowing the replacement of the native promoter of the *pmmA* gene by P_{alcA}. The fragment from −60 to +957 of the *pmmA* genomic DNA sequence was amplified with primers P7 and P8 (Table S1). The PCR-amplified fragment was cloned into the expression vector pAL3 to yield pALPmmN and confirmed by sequencing using the University of Dundee sequencing service. Generation of protoplasts and polyethylene glycol-mediated transformation were performed as previously described (Tilburn et al., 1983) and positive transformants were selected for uridine/uracil prototrophy. The transformants were confirmed by PCR and southern blotting. For PCR analysis, three pairs of primers (P1/P2, P3/P4, and P5/P6) (Table S1) were utilized. Primers P1 and P2 were used to amplify a 1,087 bp fragment of the *pmmA* gene. P3 and P4 were used to amplify a 1.59 kb fragment from the P_{alcA} to a downstream flanking region of the *pmmA* gene. Primers P5 and P6 were used to amplify the *N. crassa pyr-4* gene. For southern blot, genomic DNA of parental and *pmmA* conditional strains was digested with XbaI, separated by electrophoresis, and transferred to a nylon membrane (Zeta-probe+, Bio-Rad). The 800 bp fragment of *pmmA* was used as probe. Labeling and visualization were performed using the DIG DNA labeling and detection kit (Roche Applied Science) according to the manufacturer's instructions.

4.4 | Quantitative real-time PCR

Total RNA from *A. fumigatus* cultured in liquid MM supplemented with 0.1 M threonine (MMT) or 1% glucose (MMTG) at 37°C, 200 rpm for 48 hr was extracted using Trizol reagent (Invitrogen). Complementary DNA synthesis was performed with 1.5 μg of RNA using the qScript cDNA SuperMix (Quanta bioscience) according to the manufacturer's instruction. Primers P9 and P10 were used to amplify a fragment of *pmmA*, and Primers P11 and P12 were used to amplify an 80 bp *tbp* gene (encoding TATA-box-binding protein, as a reference gene). Quantitative real-time PCR (qRT-PCR) was carried out with the PerfeCta SYBR Green FastMix (Quanta bioscience) using a Rotor-Gene Q real-time PCR system (Qiagen). Thermal cycling conditions were 95°C for 2 min, followed by 45 cycles of 95°C for 15 s, and 60°C for 60 s. Real-time PCR data were acquired using Sequence Detection software. The standard curve method was used to analyze the real-time PCR data. Samples isolated from different strains and at different time were tested in triplicate.

4.5 | Analysis of the P_{alcA}::*pmmA* conditional mutant

To test the sensitivity of the conditional mutant to cell wall perturbing reagents, serial dilutions of P_{alcA}::*pmmA* and wild-type conidia from 10^5 to 10^2 were inoculated on MMT or MMTG plates containing 100 μg/ml Calcofluor White, 100 μg/ml Congo Red and 5 μg/ml Caspofungin, respectively. After incubation at 37°C for 48 hr, the plates were photographed.

For quantitative determination of cell wall monosaccharides, conidia were inoculated into 100 ml MMTG liquid medium at a concentration of 10^6 conidia ml^{-1} and incubated at 37°C with shaking at 200 rpm for 48 hr. The mycelia were harvested, washed with deionized water and stored at −80°C. Fungal cell wall monosaccharides were extracted and quantitatively determined as described previously (Francois, 2006). For the conidial germination assay, 1×10^6 conidia ml^{-1} were inoculated into 20 ml liquid MMTG containing a single coverslip and incubated at 37°C. Germination rate was determined by counting a total of 100 spores and noting the number of germinated spores using a bright-field microscope at each time point. Counting was repeated three times for each strain. Radial growth rate was determined by inoculating 10^4 conidia onto solid MMTG media and recording colony diameter daily. For the conidiation assay, 5 μl conidia suspensions (10^6 conidia ml^{-1}) were spotted onto solid MMTG or MMT media and incubated at 37°C for 2 days. Conidia were collected with 0.05% Tween 20 solution and quantified. Values represent means standard deviations (*SD*) of results from three different experiments.

4.6 | Western blotting

The indicated strains were inoculated into liquid MMTG and cultured at 37°C, 200 rpm for 48 hr. The mycelia were harvested and ground in liquid nitrogen with a mortar and pestle, then resuspended in lysis buffer

(10 mM Tris-HCl pH 7.5, 150 mM NaCl, 0.5 mM EDTA, 1 mM PMSF, protease inhibitor mixture), and centrifuged at 10,000*g* for 15 min at 4°C. Supernatants were collected as total proteins. Secreted proteins from culture media were concentrated by acetone precipitation. The total and secreted proteins were separated in 12% SDS-PAGE gels and then transferred into a polyvinylidene difluoride (PVDF) membrane (Millipore). The blots were probed with biotinylated ConA (1:2000, Vector Laboratories, B-1005-5) and subsequently with horseradish peroxidase-conjugated streptavidin (1:1,000, Vector Laboratories, SA-5014-1). Blots were detected by Enhanced ECL luminescence detection kit (Vazyme, E411), and images were acquired with a Tanon 4200 chemiluminescent imaging system (Tanon).

4.7 | High-pressure freeze substitution transmission electron microscopy

Strains were grown in liquid MMTG or MMT media at 37°C for 24 hr. The harvested mycelia were frozen under pressure using a Leica EM AFS2 automatic freeze substitution system and EM FSP freeze substitution processor (Leica Microsystems). The freeze substitution and embedding, sectioning, and staining was performed by the Microscopy and Histology Facility of the Institute of Medical Sciences, University of Aberdeen as described previously (Hall et al., 2013). Samples were examined using a Philips CM10 transmission microscope (FEI UK Ltd., Cambridge, United Kingdom), and images were captured using a Gatan BioScan 792 camera system (Gatan UK, Abingdon, United Kingdom). The average thicknesses of cell wall layers were calculated from 10 measurements for each strain.

4.8 | Cloning of *A. fumigatus pmmA*

The *A. fumigatus pmmA* gene (accession no. Q4WNF2) was amplified by PCR from an *A. fumigatus* cDNA library using primers P1/P2 (Table S1) for cloning into plasmid pGEX-6P1 (GE Healthcare). This generated the final expression plasmid pGEX-*Af*PmmA$_{12\text{-}269}$ (amino acids 12–269). This vector encodes a glutathione-*S*-transferase (GST) tag followed by a PreScission protease cleavage site. Site-direct mutagenesis of D25N and D27N was performed using pGEX-*Af*PmmA$_{12\text{-}269}$ as the template, P15, P16 and P17, P18 (Table S1) as primers following the QuickChange protocol (Stratagene). All plasmids were verified by sequencing using the University of Dundee sequencing service.

4.9 | Expression and purification of *Af*PmmA

The *N*-terminally truncated pGEX-*Af*PmmA$_{12\text{-}269}$ and mutated forms (D25N, D27N) were transformed into *E. coli* BL21 (DE3) pLysS and cultured in Luria–Bertani (LB) medium supplemented with ampicillin (0.1 mg/ml) at 37°C. Then, 10 ml culture was used to inoculate 1 liter LB medium and grown to an OD_{600} of 0.6. Protein expression was induced by 250 μM of IPTG (isopropyl-β-D-thiogalactopyranoside) and then incubated at 16°C for 18 hr. The cells were harvested by centrifugation at 3,500 rpm, 4°C for 30 min. The cell pellet was re-suspended in 25 ml of ice-cold lysis buffer containing 25 mM HEPES pH 7.5, 150 mM NaCl, 10 mg/ml DNase, 0.5 mg/ml lysozyme and a tablet of protease inhibitor cocktail (Roche) and lysed using a French press at 600 psi. After centrifugation (20,000*g*, 30 min, 4°C), the supernatant was incubated with pre-washed glutathione Sepharose 4B beads (GE Healthcare) at 4°C on a rotating platform for 2 hr and subsequently the GST tag was cleaved with PreScission protease by incubating at 4°C for 18 hr. The eluted solution was concentrated to 5 ml using a 10 kDa cut-off Vivaspin concentrator (GE Healthcare) and loaded onto a Superdex 200 column (Amersham Bioscience) equilibrated with the same lysis buffer and eluted at a flow rate of 1 ml/min. The fractions were concentrated using a 10 kDa cut-off Vivaspin concentrator (GE Healthcare) and verified by 10% SDS-PAGE.

4.10 | Steady-state kinetics

A. fumigatus PmmA activity was determined via a coupled fluorescent assay as reported previously (Pirard, Achouri, et al., 1999) with minor modifications. Briefly, 10 μM glucose-1,6-bisphosphate was used as the co-factor and the reaction mixture was incubated at 30°C for 30 min in a buffer consisting of 50 mM HEPES pH 7.1, 5 mM $MgCl_2$, 0.25 mM $NADP^+$ and 10 μg/ml glucose-6-phosphate dehydrogenase. Phosphoglucomutase activity was measured in the presence of 0 to 500 μM glucose 1-phosphate, and phosphomannomutase activity was measured in the presence of 0 to 300 μM mannose-1-phosphate using 10 μg/ml of phosphoglucose isomerase (Pgi) and 3.5 μg/ml of phosphomannose isomerase (Pmi), respectively. The production of NADPH was determined using a SpectraMax i3x (Molecular Devices) with emission at 440 nm and excitation at 340 nm. To detect the effects of divalent metal ions on *Af*PmmA activity, 1 mM EDTA and 5 mM each metal ion (Mg^{2+}, Ca^{2+}, Mn^{2+}, Zn^{2+}) were added and the activities were measured using 200 μM Glc-1P as substrate.

4.11 | Crystallization, data collection, and structure determination

Sixteen milligram per milliliters of pure *Af*PmmA protein in 25 mM HEPES buffer, 150 mM NaCl, pH 7.5 was used for crystal screening using the sitting drop method. Each drop contained an equal volume of 0.2 μl of protein and 0.2 μl of reservoir solution. Crystals grew after 3 days from condition C1 of Morpheus Screen HT-96 (0.09 M NPS, 0.1 M MES/Imidazole pH 6.5, 20% v/v PEG500 MME, 10% w/v PEG 20,000) (Molecular Dimension). Data were collected on a Rigaku Saturn 944 + CCD with a Rigaku MM007 HFM generator (wavelength 1.54 Å) at 100 K using 0.25 oscillations for 188 images and processed with the HKL suite (Otwinowski & Minor, 1997). The

structure was solved by molecular replacement using MOLREP with the *Hs*Pmm1-Man-1P complex structure (PDB entry 2FUE, Silvaggi et al., 2006) as the search model. REFMAC (Murshudov et al., 1997) was used for further refinement and iterated with model building using COOT (Emsley & Cowtan, 2004). Figures were produced with PyMol (DeLano, 2004). The atomic co-ordinates and structure factors of *Af*PmmA were deposited in the Protein Data Bank with accession code 6I5X.

ACKNOWLEDGMENTS

This work was funded by an MRC Programme Grant (M004139) to D.M.F.v.A. Y.Z. is funded by a China Scholarship Council PhD studentship, National Natural Science Foundation of China (31900404) and Natural Science Foundation of the Jiangsu Higher Education Institutions of China (19KJB180017). D.L. is supported by a Wellcome Trust Postdoctoral Research Training Fellowship for Clinicians (105772/Z/14/Z). W.F. is funded by Guangxi Natural Science Foundation (2018GXNSFAA138012) and National Natural Science Foundation of China (31960032).

CONFLICT OF INTEREST

The authors declare that they have no conflict of interests.

AUTHOR CONTRIBUTIONS

Y.Z. and D.M.F.v.A conceived the study; Y.Z., O.G.R. performed experiments; A.T.F. performed molecular biology; Y.Z., W.F. and D.M.F.v.A. analyzed data and Y.Z., D.L., L.L. and D.M.F.v.A. interpreted the data and wrote the manuscript with input from all authors.

DATA AVAILABILITY STATEMENT

The atomic co-ordinates and structure factors of AfPmmA were deposited in the Protein Data Bank with accession code 6I5X.

ORCID

Yuanwei Zhang https://orcid.org/0000-0003-0854-6123
Daan M. F. van Aalten https://orcid.org/0000-0002-1499-6908

REFERENCES

Allen, K.N. & Dunaway-Mariano, D. (2004) Phosphoryl group transfer: Evolution of a catalytic scaffold. *Trends in Biochemical Sciences*, *29*, 495–503. Available from: https://doi.org/10.1016/j.tibs.2004.07.008.

Armitt, S., McCullough, W. & Roberts, C.F. (1976) Analysis of acetate non-utilizing (acu) mutants in *Aspergillus nidulans*. *Journal of General Microbiology*, *92*, 263–282. Available from: https://doi.org/10.1099/00221287-92-2-263.

Barreto-Bergter, E. & Figueiredo, R.T. (2014) Fungal glycans and the innate immune recognition. *Frontiers in Cellular and Infection Microbiology*, *4*, 145. Available from: https://doi.org/10.3389/fcimb.2014.00145.

Bell, A.S., Mills, J.E., Williams, G.P., Brannigan, J.A., Wilkinson, A.J., Parkinson, T. et al. (2012) Selective inhibitors of protozoan protein N-myristoyltransferases as starting points for tropical disease medicinal chemistry programs. *PLoS Neglected Tropical Diseases*, *6*, e1625. Available from: https://doi.org/10.1371/journal.pntd.0001625.

Bernard, M. & Latge, J.P. (2001) *Aspergillus fumigatus* cell wall: Composition and biosynthesis. *Medical Mycology*, *39*(Suppl 1), 9–17.

Bongomin, F., Gago, S., Oladele, R.O. & Denning, D.W. (2017) Global and multi-national prevalence of fungal diseases-estimate precision. *Journal of Fungi (Basel)*, *3*, 57. Available from: https://doi.org/10.3390/jof3040057.

Bowman, S.M. & Free, S.J. (2006) The structure and synthesis of the fungal cell wall. *BioEssays*, *28*, 799–808. Available from: https://doi.org/10.1002/bies.20441.

Brown, G.D., Denning, D.W., Gow, N.A., Levitz, S.M., Netea, M.G. & White, T.C. (2012) Hidden killers: Human fungal infections. *Science Translational Medicine*, *4*, 165rv113. Available from: https://doi.org/10.1126/scitranslmed.3004404.

Calderone, R., Sun, N., Gay-Andrieu, F., Groutas, W., Weerawarna, P., Prasad, S. et al. (2014) Antifungal drug discovery: The process and outcomes. *Future Microbiology*, *9*, 791–805. Available from: https://doi.org/10.2217/fmb.14.32.

Casadevall, A. & Pirofski, L.A. (2003) The damage-response framework of microbial pathogenesis. *Nature Reviews Microbiology*, *1*, 17–24. Available from: https://doi.org/10.1038/nrmicro732.

Collet, J.F., Stroobant, V., Pirard, M., Delpierre, G. & Van Schaftingen, E. (1998) A new class of phosphotransferases phosphorylated on an aspartate residue in an amino-terminal DXDX(T/V) motif. *Journal of Biological Chemistry*, *273*, 14107–14112. Available from: https://doi.org/10.1074/jbc.273.23.14107.

Cromphout, K., Vleugels, W., Heykants, L., Schollen, E., Keldermans, L., Sciot, R. et al. (2006) The normal phenotype of Pmm1-deficient mice suggests that Pmm1 is not essential for normal mouse development. *Molecular and Cellular Biology*, *26*, 5621–5635. Available from: https://doi.org/10.1128/MCB.02357-05.

da Silva Ferreira, M.E., Kress, M.R., Savoldi, M., Goldman, M.H., Hartl, A., Heinekamp, T. et al. (2006) The akuB(KU80) mutant deficient for nonhomologous end joining is a powerful tool for analyzing pathogenicity in *Aspergillus fumigatus*. *Eukaryotic Cell*, *5*, 207–211. Available from: https://doi.org/10.1128/EC.5.1.207-211.2006.

De Groot, P.W., Ram, A.F. & Klis, F.M. (2005) Features and functions of covalently linked proteins in fungal cell walls. *Fungal Genetics and Biology*, *42*, 657–675. Available from: https://doi.org/10.1016/j.fgb.2005.04.002.

DeLano, W.L. (2004) Use of PYMOL as a communications tool for molecular science. *Abstracts of Papers of the American Chemical Society*, *228*, U313–U314.

d'Enfert, C. (1996) Selection of multiple disruption events in *Aspergillus fumigatus* using the orotidine-5'-decarboxylase gene, *pyrG*, as a unique transformation marker. *Current Genetics*, *30*, 76–82. Available from: https://doi.org/10.1007/s002940050103.

Denning, D.W. & Bromley, M.J. (2015) Infectious disease. How to bolster the antifungal pipeline. *Science*, *347*, 1414–1416. Available from: https://doi.org/10.1126/science.aaa6097.

Emsley, P. & Cowtan, K. (2004) Coot: Model-building tools for molecular graphics. *Acta Crystallographica Section D, Biological Crystallography*, *60*, 2126–2132.

Engel, J., Schmalhorst, P.S. & Routier, F.H. (2012) Biosynthesis of the fungal cell wall polysaccharide galactomannan requires intraluminal GDP-mannose. *Journal of Biological Chemistry*, *287*, 44418–44424. Available from: https://doi.org/10.1074/jbc.M112.398321.

Erlanson, D.A., Fesik, S.W., Hubbard, R.E., Jahnke, W. & Jhoti, H. (2016) Twenty years on: The impact of fragments on drug discovery. *Nature Reviews Drug Discovery*, *15*, 605–619. Available from: https://doi.org/10.1038/nrd.2016.109.

Fang, W., Du, T., Raimi, O.G., Hurtado-Guerrero, R., Marino, K., Ibrahim, A.F. et al. (2013a) Genetic and structural validation of *Aspergillus fumigatus* N-acetylphosphoglucosamine mutase as an antifungal target. *Bioscience Reports*, *33*, e00063. Available from: https://doi.org/10.1042/BSR20130053.

Fang, W., Du, T., Raimi, O.G., Hurtado-Guerrero, R., Urbaniak, M.D., Ibrahim, A.F. et al. (2013b) Genetic and structural validation of *Aspergillus fumigatus* UDP-N-acetylglucosamine pyrophosphorylase as an antifungal target. *Molecular Microbiology*, *89*, 479–493.

Fang, W., Yu, X., Wang, B., Zhou, H., Ouyang, H., Ming, J. et al. (2009) Characterization of the *Aspergillus fumigatus* phosphomannose isomerase Pmi1 and its impact on cell wall synthesis and morphogenesis. *Microbiology*, *155*, 3281–3293. Available from: https://doi.org/10.1099/mic.0.029975-0.

Francois, J.M. (2006) A simple method for quantitative determination of polysaccharides in fungal cell walls. *Nature Protocols*, *1*, 2995–3000. Available from: https://doi.org/10.1038/nprot.2006.457.

Garami, A., Mehlert, A. & Ilg, T. (2001) Glycosylation defects and virulence phenotypes of *Leishmania mexicana* phosphomannomutase and dolicholphosphate-mannose synthase gene deletion mutants. *Molecular and Cellular Biology*, *21*, 8168–8183. Available from: https://doi.org/10.1128/MCB.21.23.8168-8183.2001.

Gow, N.A.R., Latge, J.P. & Munro, C.A. (2017) The fungal cell wall: Structure, biosynthesis, and function. *Microbiology Spectrum*, *5*, 1–25.

Grunewald, S. (2009) The clinical spectrum of phosphomannomutase 2 deficiency (CDG-Ia). *Biochimica et Biophysica Acta*, *1792*, 827–834. Available from: https://doi.org/10.1016/j.bbadis.2009.01.003.

Hall, R.A., Bates, S., Lenardon, M.D., Maccallum, D.M., Wagener, J., Lowman, D.W. et al. (2013) The Mnn2 mannosyltransferase family modulates mannoprotein fibril length, immune recognition and virulence of *Candida albicans*. *PLoS Pathogens*, *9*, e1003276. Available from: https://doi.org/10.1371/journal.ppat.1003276.

Henry, C., Li, J., Danion, F., Alcazar-Fuoli, L., Mellado, E., Beau, R. et al. (2019) Two KTR mannosyltransferases are responsible for the biosynthesis of cell wall mannans and control polarized growth in *Aspergillus fumigatus*. *mBio*, *10*, e02647-18.

Hoeberichts, F.A., Vaeck, E., Kiddle, G., Coppens, E., van de Cotte, B., Adamantidis, A. et al. (2008) A Temperature-sensitive mutation in the *Arabidopsis thaliana* phosphomannomutase gene disrupts protein glycosylation and triggers cell death. *Journal of Biological Chemistry*, *283*, 5708–5718. Available from: https://doi.org/10.1074/jbc.M704991200.

Hu, W., Sillaots, S., Lemieux, S., Davison, J., Kauffman, S., Breton, A. et al. (2007) Essential gene identification and drug target prioritization in *Aspergillus fumigatus*. *PLoS Pathogens*, *3*, e24. Available from: https://doi.org/10.1371/journal.ppat.0030024.

Ji, T., Zhang, C., Zheng, L., Dunaway-Mariano, D. & Allen, K.N. (2018) Structural basis of the molecular switch between phosphatase and mutase functions of human phosphomannomutase 1 under ischemic conditions. *Biochemistry*, *57*, 3480–3492. Available from: https://doi.org/10.1021/acs.biochem.8b00223.

Jiang, H., Ouyang, H., Zhou, H. & Jin, C. (2008) GDP-mannose pyrophosphorylase is essential for cell wall integrity, morphogenesis and viability of *Aspergillus fumigatus*. *Microbiology (Reading)*, *154*, 2730–2739. Available from: https://doi.org/10.1099/mic.0.2008/019240-0.

Jin, C. (2012) Protein glycosylation in *Aspergillus fumigatus* is essential for cell wall synthesis and serves as a promising model of multicellular eukaryotic development. *International Journal of Microbiology*, *2012*, 654251.

Jin, Y., Bhattasali, D., Pellegrini, E., Forget, S.M., Baxter, N.J., Cliff, M.J. et al. (2014) alpha-Fluorophosphonates reveal how a phosphomutase conserves transition state conformation over hexose recognition in its two-step reaction. *Proceedings of the National Academy of Sciences of the United States of America*, *111*, 12384–12389. Available from: https://doi.org/10.1073/pnas.1402850111.

Kahn, J.N., Hsu, M.J., Racine, F., Giacobbe, R. & Motyl, M. (2006) Caspofungin susceptibility in *Aspergillus* and non-*Aspergillus* molds: Inhibition of glucan synthase and reduction of beta-D-1,3 glucan levels in culture. *Antimicrobial Agents and Chemotherapy*, *50*, 2214–2216.

Kedzierski, L., Malby, R.L., Smith, B.J., Perugini, M.A., Hodder, A.N., Ilg, T. et al. (2006) Structure of *Leishmania mexicana* phosphomannomutase highlights similarities with human isoforms. *Journal of Molecular Biology*, *363*, 215–227. Available from: https://doi.org/10.1016/j.jmb.2006.08.023.

Kepes, F. & Schekman, R. (1988) The yeast *SEC53* gene encodes phosphomannomutase. *Journal of Biological Chemistry*, *263*, 9155–9161. Available from: https://doi.org/10.1016/S0021-9258(19)76520-X.

Knowles, J.R. (1980) Enzyme-catalyzed phosphoryl transfer reactions. *Annual Review of Biochemistry*, *49*, 877–919. Available from: https://doi.org/10.1146/annurev.bi.49.070180.004305.

Kousha, M., Tadi, R. & Soubani, A.O. (2011) Pulmonary aspergillosis: A clinical review. *European Respiratory Reviews*, *20*, 156–174. Available from: https://doi.org/10.1183/09059180.00001011.

Latge, J.P., Beauvais, A. & Chamilos, G. (2017) The cell wall of the human fungal pathogen *Aspergillus fumigatus*: Biosynthesis, organization, immune response, and virulence. *Annual Review of Microbiology*, *71*, 99–116.

Latge, J.P., Mouyna, I., Tekaia, F., Beauvais, A., Debeaupuis, J.P. & Nierman, W. (2005) Specific molecular features in the organization and biosynthesis of the cell wall of *Aspergillus fumigatus*. *Medical Mycology*, *43*(Suppl 1), S15–S22.

Lee, M.J. & Sheppard, D.C. (2016) Recent advances in the understanding of the *Aspergillus fumigatus* cell wall. *Journal of Microbiology*, *54*, 232–242. Available from: https://doi.org/10.1007/s12275-016-6045-4.

Li, M., Chen, T., Gao, T., Miao, Z., Jiang, A., Shi, L. et al. (2015) UDP-glucose pyrophosphorylase influences polysaccharide synthesis, cell wall components, and hyphal branching in *Ganoderma lucidum* via regulation of the balance between glucose-1-phosphate and UDP-glucose. *Fungal Genetics and Biology*, *82*, 251–263. Available from: https://doi.org/10.1016/j.fgb.2015.07.012.

Liu, H.Y., Wang, Z., Regni, C., Zou, X. & Tipton, P.A. (2004) Detailed kinetic studies of an aggregating inhibitor; inhibition of phosphomannomutase/phosphoglucomutase by disperse blue 56. *Biochemistry*, *43*, 8662–8669.

Lockhart, D.E.A., Stanley, M., Raimi, O.G., Robinson, D.A., Boldovjakova, D., Squair, D.R. et al. (2020) Targeting a critical step in fungal hexosamine biosynthesis. *Journal of Biological Chemistry*, *295*, 8678–8691. Available from: https://doi.org/10.1074/jbc.RA120.012985.

Murshudov, G.N., Vagin, A.A. & Dodson, E.J. (1997) Refinement of macromolecular structures by the maximum-likelihood method. *Acta Crystallographica Section D, Biological Crystallography*, *53*, 240–255. Available from: https://doi.org/10.1107/S0907444996012255.

Nogly, P., Matias, P.M., de Rosa, M., Castro, R., Santos, H., Neves, A.R. et al. (2013) High-resolution structure of an atypical alpha-phosphoglucomutase related to eukaryotic phosphomannomutases. *Acta Crystallographica Section D, Biological Crystallography*, *69*, 2008–2016.

Onoue, T., Tanaka, Y., Hagiwara, D., Ekino, K., Watanabe, A., Ohta, K. et al. (2018) Identification of two mannosyltransferases contributing to biosynthesis of the fungal-type galactomannan alpha-core-mannan structure in *Aspergillus fumigatus*. *Scientific Reports*, *8*, 16918.

Osmani, A.H., Oakley, B.R. & Osmani, S.A. (2006) Identification and analysis of essential *Aspergillus nidulans* genes using the heterokaryon rescue technique. *Nature Protocols*, *1*, 2517–2526. Available from: https://doi.org/10.1038/nprot.2006.406.

Ostrosky-Zeichner, L., Casadevall, A., Galgiani, J.N., Odds, F.C. & Rex, J.H. (2010) An insight into the antifungal pipeline: Selected new molecules and beyond. *Nature Reviews Drug Discovery*, *9*, 719–727. Available from: https://doi.org/10.1038/nrd3074.

Otwinowski, Z. & Minor, W. (1997) Processing of X-ray diffraction data collected in oscillation mode. *Methods in Enzymology*, *276*, 307–326.

Pirard, M., Achouri, Y., Collet, J.F., Schollen, E., Matthijs, G. & Van Schaftingen, E. (1999) Kinetic properties and tissular distribution of mammalian phosphomannomutase isozymes. *The Biochemical Journal*, *339*(Pt 1), 201–207. Available from: https://doi.org/10.1042/bj3390201.

Pirard, M., Matthijs, G., Heykants, L., Schollen, E., Grunewald, S., Jaeken, J. et al. (1999) Effect of mutations found in carbohydrate-deficient glycoprotein syndrome type IA on the activity of phosphomannomutase 2. *FEBS Letters*, *452*, 319–322. Available from: https://doi.org/10.1016/S0014-5793(99)00673-0.

Qian, W., Yu, C., Qin, H., Liu, X., Zhang, A., Johansen, I.E. et al. (2007) Molecular and functional analysis of phosphomannomutase (PMM) from higher plants and genetic evidence for the involvement of PMM in ascorbic acid biosynthesis in *Arabidopsis* and *Nicotiana benthamiana*. *The Plant Journal*, *49*, 399–413. Available from: https://doi.org/10.1111/j.1365-313X.2006.02967.x.

Rackham, M.D., Brannigan, J.A., Rangachari, K., Meister, S., Wilkinson, A.J., Holder, A.A. et al. (2014) Design and synthesis of high affinity inhibitors of *Plasmodium falciparum* and *Plasmodium vivax* N-myristoyltransferases directed by ligand efficiency dependent lipophilicity (LELP). *Journal of Medicinal Chemistry*, *57*, 2773–2788.

Ram, A.F. & Klis, F.M. (2006) Identification of fungal cell wall mutants using susceptibility assays based on Calcofluor white and Congo red. *Nature Protocols*, *1*, 2253–2256. Available from: https://doi.org/10.1038/nprot.2006.397.

Rao, S.T. & Rossmann, M.G. (1973) Comparison of super-secondary structures in proteins. *Journal of Molecular Biology*, *76*, 241–256. Available from: https://doi.org/10.1016/0022-2836(73)90388-4.

Robbins, N., Caplan, T. & Cowen, L.E. (2017) Molecular evolution of antifungal drug resistance. *Annual Review of Microbiology*, *71*, 753–775. Available from: https://doi.org/10.1146/annurev-micro-030117-020345.

Romero, B., Turner, G., Olivas, I., Laborda, F. & De Lucas, J.R. (2003) The *Aspergillus nidulans alcA* promoter drives tightly regulated conditional gene expression in *Aspergillus fumigatus* permitting validation of essential genes in this human pathogen. *Fungal Genetics and Biology*, *40*, 103–114. Available from: https://doi.org/10.1016/S1087-1845(03)00090-2.

Scott, D.E., Coyne, A.G., Hudson, S.A. & Abell, C. (2012) Fragment-based approaches in drug discovery and chemical biology. *Biochemistry*, *51*, 4990–5003. Available from: https://doi.org/10.1021/bi3005126.

Seifried, A., Schultz, J. & Gohla, A. (2013) Human HAD phosphatases: Structure, mechanism, and roles in health and disease. *FEBS Journal*, *280*, 549–571. Available from: https://doi.org/10.1111/j.1742-4658.2012.08633.x.

Sharma, V., Ichikawa, M. & Freeze, H.H. (2014) Mannose metabolism: More than meets the eye. *Biochemical and Biophysical Research Communications*, *453*, 220–228. Available from: https://doi.org/10.1016/j.bbrc.2014.06.021.

Silvaggi, N.R., Zhang, C., Lu, Z., Dai, J., Dunaway-Mariano, D. & Allen, K.N. (2006) The X-ray crystal structures of human alpha-phosphomannomutase 1 reveal the structural basis of congenital disorder of glycosylation type 1a. *Journal of Biological Chemistry*, *281*, 14918–14926.

Staneva, D., Uccelletti, D., Farina, F., Venkov, P. & Palleschi, C. (2004) *KISEC53* is an essential *Kluyveromyces lactis* gene and is homologous with the *SEC53* gene of *Saccharomyces cerevisiae*. *Yeast*, *21*, 41–51. Available from: https://doi.org/10.1002/yea.1055.

Thiel, C., Lubke, T., Matthijs, G., von Figura, K. & Korner, C. (2006) Targeted disruption of the mouse phosphomannomutase 2 gene causes early embryonic lethality. *Molecular and Cellular Biology*, *26*, 5615–5620. Available from: https://doi.org/10.1128/MCB.02391-05.

Tilburn, J., Scazzocchio, C., Taylor, G.G., Zabicky-Zissman, J.H., Lockington, R.A. & Davies, R.W. (1983) Transformation by integration in *Aspergillus nidulans*. *Gene*, *26*, 205–221. Available from: https://doi.org/10.1016/0378-1119(83)90191-9.

Todd, R.B., Davis, M.A. & Hynes, M.J. (2007) Genetic manipulation of *Aspergillus nidulans*: Meiotic progeny for genetic analysis and strain construction. *Nature Protocols*, *2*, 811–821. Available from: https://doi.org/10.1038/nprot.2007.112.

Upadhyay, S. & Shaw, B.D. (2006) A phosphoglucose isomerase mutant in *Aspergillus nidulans* is defective in hyphal polarity and conidiation. *Fungal Genetics and Biology*, *43*, 739–751. Available from: https://doi.org/10.1016/j.fgb.2006.05.002.

Urbaniak, M.D., Collie, I.T., Fang, W., Aristotelous, T., Eskilsson, S., Raimi, O.G. et al. (2013) A novel allosteric inhibitor of the uridine diphosphate N-acetylglucosamine pyrophosphorylase from *Trypanosoma brucei*. *ACS Chemical Biology*, *8*, 1981–1987.

Westphal, V., Peterson, S., Patterson, M., Tournay, A., Blumenthal, A., Treacy, E.P. et al. (2001) Functional significance of PMM2 mutations in mildly affected patients with congenital disorders of glycosylation Ia. *Genetics in Medicine*, *3*, 393–398. Available from: https://doi.org/10.1097/00125817-200111000-00003.

Zhang, P., Wei, D., Li, Z., Sun, Z., Pan, J. & Zhu, X. (2015) Cryptococcal phosphoglucose isomerase is required for virulence factor production, cell wall integrity and stress resistance. *FEMS Yeast Research*, *15*, fov072. Available from: https://doi.org/10.1093/femsyr/fov072.

Zou, Y., Ma, D. & Wang, Y. (2019) The PROTAC technology in drug development. *Cell Biochemistry and Function*, *37*, 21–30. Available from: https://doi.org/10.1002/cbf.3369.

SUPPORTING INFORMATION

Additional Supporting Information may be found online in the Supporting Information section.

How to cite this article: Zhang Y, Fang W, Raimi OG, et al. Genetic and structural validation of phosphomannomutase as a cell wall target in *Aspergillus fumigatus*. *Mol Microbiol*. 2021;00:1–15. https://doi.org/10.1111/mmi.14706